

# Reinforcement Learning with Elastic Time Steps\*

Dong Wang<sup>1</sup>, Giovanni Beltrame<sup>1,\*</sup>

<sup>a</sup>*Polytechnique Montréal, 2500, chemin de Polytechnique, H3T 1J4, Montréal (Québec), Canada*

## Abstract

Traditional Reinforcement Learning (RL) policies are typically implemented with fixed control rates, often disregarding the impact of control rate selection. This can lead to inefficiencies as the optimal control rate varies with task requirements. We present the Multi-Objective Soft Elastic Actor-Critic (MOSEAC), an off-policy actor-critic algorithm that uses elastic time steps to dynamically adjust the control frequency. This technique minimizes computational resources by selecting the lowest viable frequency. We demonstrate that MOSEAC converges and produces stable policies at the theoretical level, and validate our findings in a real-time 3D racing game. MOSEAC significantly outperformed other variable time step approaches in terms of energy efficiency and task effectiveness. Additionally, MOSEAC shown faster and more stable training, showcasing its potential for real-world RL applications in robotics.

**Keywords:** Reinforcement Learning, Learning and Adaptive Systems, Optimization and Optimal Control

## 1. Introduction

Model-free deep Reinforcement Learning (DRL) has shown notable value in diverse domains, from video games [23, 25] to robotic control [10, 29]. For example, Sony’s autonomous racing cars achieved remarkable results with fixed training frequencies of 10 Hz and 60 Hz [29].

However, suboptimal fixed control rates present limitations, leading to excessive caution, wasted computational resources, risky behavior, and compromised control.

Variable Time Step Reinforcement Learning (VTS-RL) has been introduced to address these issues in traditional RL by utilizing reactive programming principles [16, 4]. VTS-RL performs control actions only when necessary, reducing computational load and enabling variable action durations. For example, in robotic manipulation, VTS-RL allows a robot arm to dynamically adjust its control frequency, utilizing lower frequencies for simple tasks and higher frequencies for complex maneuvers or delicate handling [11].

Two notable VTS-RL algorithms are Soft Elastic Actor-Critic (SEAC) [26] and Continuous-Time Continuous-Options (CTCO) [11]. CTCO supports continuous-time decision-making with flexible option durations, enhancing exploration and robustness. However, it requires tuning multiple hyperparameters, such as radial basis functions (RBFs) and time-related parameters  $\tau$  for its adaptive discount factor  $\gamma$ , making tuning complex in certain environments.

SEAC incorporates reward components related to task energy (number of actions) and task time, making it effective in

time-constrained environments. Despite its advantages, SEAC requires careful tuning of hyperparameters to balance task, energy, and time costs to ensure optimal performance. The sensitivity of both SEAC and CTCO to hyperparameter settings presents a challenge for users aiming to fully exploit their capabilities.

We recently proposed Multi-Objective Soft Elastic Actor-Critic (MOSEAC [27]), which reduced the dimension of hyperparameters and the algorithm’s dependence on hyperparameters by dynamically adjusting the hyperparameters corresponding to the reward structure.

We identify shortcomings in our previous work, where we proposed adapting  $\alpha_m$  by monitoring reward trends. However, in some tasks, reward trends are not always stable, posing a risk of reward explosion. To address this, we introduce an upper limit  $\alpha_{max}$  for  $\alpha_m$ . We provide pseudocode for this improvement and established a corresponding Lyapunov stability function [15] to demonstrate the stability (convergence) of the new algorithm.

We evaluate MOSEAC in a racing game (Ubisoft TrackMania [1]), comparing it against CTCO [11], SEAC [26] and Soft Actor-Critic (SAC [9]). Our results demonstrate MOSEAC’s improved training speed, stability, and efficiency. Our key contributions are:

- Algorithm Enhancement and Convergence Proof:** We introduce an upper limit  $\alpha_{max}$  on the parameter  $\alpha_m$  to prevent reward explosion, ensuring the stability and convergence of the MOSEAC algorithm. This enhancement is validated through a Lyapunov model, providing a proof of convergence and demonstrating the efficacy of the new adjustment mechanism.
- Enhanced Training Efficiency:** We demonstrate that MOSEAC achieves faster and more stable training than CTCO, highlighting its practical benefits and applicabil-

\*This work was partly presented at the Finding the Frame Workshop in August 2024.

\*Corresponding author

Email addresses: dong-1.wang@polymtl.ca (Dong Wang), giovanni.beltrame@polymtl.ca (Giovanni Beltrame)

ity in real-world scenarios.

The paper is organized as follows. Section 2 describes the current research status of variable time step RL. Section 3 introduces MOSEAC with its pseudocode and Lyapunov model. Section 4 describes the test environments. Section 5 presents the simulation parameters and results. Finally, Section 6 concludes the paper.

## 2. Related Work

Fixed control rates in RL often lead to inefficiencies. Research by [26] shows that suboptimal fixed rates can cause excessive caution or risky behavior, wasting resources and compromising control. Control rates significantly impact continuous control systems beyond computational demands. Some studies [2, 19] indicate that high control rates can degrade RL performance, while low rates hinder adaptability in complex scenarios.

Sharma et al. [21] proposed learning to repeat actions to mimic dynamic control rates, but this technique does not change the control frequency or reduce computational demands. Few studies have explored repetitive behaviors in real-world scenarios, such as those by Metelli et al. [17] and Lee et al. [13]. Chen et al. [5] introduced variable “control rates” utilizing actions like “sleep,” but still involved fixed-frequency checks.

Cui et al. [7] applied the Lyapunov model to verify the stability of RL algorithms and addressed handling the dynamics of power systems over time, although it still uses a fixed frequency to scan system states.

Introducing time steps of variable duration allows a robotic system to better adapt to its task and environment by adjusting control actions based on the system’s current conditions, addressing the nonlinearity and time-variant dynamics typical in robotics [22]. This adaptability ensures optimal performance through efficient resource utilization and effective response to varying conditions [3, 4].

Lyapunov models provide robust stability guarantees by employing a scalar function that decreases over time, ensuring system convergence to a desired equilibrium. By incorporating Lyapunov stability into our RL system, we ensure that the learning process remains stable, thereby preventing erratic behavior and potential system failure [7, 6].

## 3. Multi-Objective Soft Elastic Actor and Critic

Our algorithm builds upon previous work [27], combining SEAC’s hyperparameters for balancing task, energy, and time rewards through a simple multiplication technique, and applying adaptive adjustments to the remaining hyperparameters. A key improvement is the introduction of an upper limit for the hyperparameter  $\alpha_m$ . Below is an overview of the MOSEAC algorithm. This overview emphasizes the critical aspects of MOSEAC without delving into the detailed definitions. The reader can refer to [27] for details.

The reward in MOSEAC is:

$$R = \alpha_m R_t R_\tau - \alpha_\varepsilon \quad (1)$$

where  $R_t$  is the task reward,  $R_\tau$  is a time-dependent term,  $\alpha_m$  is a weighting factor to modulate reward magnitude, and  $\alpha_\varepsilon = 0.2 \cdot \left(1 - \frac{1}{1+e^{-\alpha_m+1}}\right)$  is a penalty parameter applied at each time step to reduce unnecessary actions.

To automatically set  $\alpha_m$  to an optimal value, we dynamically adjust it during training. This adjustment mitigates convergence issues, specifically the problem of sparse rewards caused by suboptimal settings of  $\alpha_m$ . MOSEAC increases  $\alpha_m$  (and decrease  $\alpha_\varepsilon$ ) if the average reward is declining.

We introduce a hyperparameter  $\psi$  to dynamically adjust  $\alpha_m$  based on observed trends in task rewards:

$$\alpha_m = \begin{cases} \alpha_m + \psi & \text{if } \alpha_m < \alpha_{max} \\ \alpha_m = \alpha_{max} & \text{otherwise} \end{cases} \quad (2)$$

In this work, we add  $\alpha_{max}$  to ensure convergence and prevent reward explosion.

Algorithm 1 presents the pseudocode for MOSEAC. MOSEAC extends the SAC algorithm by incorporating action duration  $D$  into the action policy set, enabling it to predict both the action and its duration simultaneously. The reward is computed utilizing Equation 1 and is continuously monitored. If the reward trend declines,  $\alpha_m$  increases linearly at a rate of  $\psi$ , but does not exceed  $\alpha_{max}$ . The action and critic networks are periodically updated, similar to the SAC algorithm, based on these preprocessed rewards.

The maximum number of training steps is denoted as  $t_{max}$  [24], while  $k_{length}$  indicates the maximum number of exploration steps per episode [24]. The initial random exploration phase comprises  $k_{init}$  steps [24].  $k_{update}$  [24] is the update interval determining the frequency of updates for these neural networks used in the actor and critic policies. The reward  $R_i$  is computed as  $R(S_i, A_i, D_i)$ , where  $D_i$  falls within the interval  $[D_{min}, D_{max}]$ , representing the duration of the action.

Our algorithm employs a scalarizing strategy to optimize multiple objectives, sweeping the design space by adapting  $\alpha_m$  during training. Unlike Hierarchical Reinforcement Learning (HRL) [8, 14] which aims for Pareto optimality [18] through layered reward policies, our technique simplifies the process. We focus on ease of use and computational efficiency, ensuring our technique can easily adapt to various algorithms.

It is important to note that the choice of  $\psi$  is crucial for optimal performance, as  $\psi$  represents the sweeping step of our optimization (similar to the learning parameter in gradient descent). We suggest utilizing the pre-set  $\psi$  value from our implementation to minimize the need for further adjustments. If training performance is inadequate, a high  $\psi$  value might cause the reward signal’s gradient to change too quickly, leading to instability; in this case, a lower  $\psi$  is recommended. Conversely, if training progresses too slowly, a low  $\psi$  value might weaken the reward signal, hindering convergence; thus, increasing  $\psi$  could be beneficial.

---

**Algorithm 1: Multi-Objective Soft Elastic Actor and Critic**


---

**Require:** a policy  $\pi$  with a set of parameters  $\theta, \theta'$ , critic parameters  $\phi, \phi'$ , variable time step environment model  $\Omega$ , learning-rate  $\lambda_p, \lambda_q$ , reward buffer  $\beta_r$ , replay buffer  $\beta$ .

```

1: Initialization  $i = 0, t_i = 0, \beta_r = 0$ , observe  $S_0$ 
2: while  $t_i \leq t_{max}$  do
3:   for  $i \leq k_{length} \vee \text{Not Done}$  do
4:      $A_i, D_i = \pi_\theta(S_i)$ 
5:      $S_{i+1}, R_i = \Omega(A_i, D_i)$ 
6:      $i \leftarrow i + 1$ 
7:   end
8:    $\beta_r \leftarrow 1/i \times \sum_0^i R_i$ 
9:    $\beta \leftarrow S_{0 \sim i}, A_{0 \sim i}, D_{0 \sim i}, R_{0 \sim i}, S_{1 \sim i+1}$ 
10:   $i = 0$ 
11:   $t_i \leftarrow t_i + 1$ 
12:  if  $t_i \geq k_{init}$  &  $t_i \mid k_{update}$  then
13:    Sample  $S, A, D, R, S'$  from  $(\beta)$ 
14:     $\phi \leftarrow \phi - \lambda_q \nabla_\phi \mathcal{L}_Q(\phi, S, A, D, R, S')$ 
15:     $\rightarrow$  critic update
16:     $\theta \leftarrow \theta - \lambda_p \nabla_\theta \mathcal{L}_\pi(\theta, S, A, D, \phi)$ 
17:     $\rightarrow$  actor update
18:    if  $k_R(\beta_r)$  then
19:       $\alpha_m = \alpha_m + \psi$  if  $\alpha_m < \alpha_{max}$ 
20:      Or  $\alpha_m = \alpha_{max}$  otherwise
21:       $\alpha_\varepsilon \leftarrow F_{update}(\alpha_m)$ 
22:    end
23:     $\beta_r = 0$ 
24:     $\rightarrow$  Re-record average reward values under new hyperparameters
25:  end
26:  Perform soft-update of  $\phi'$  and  $\theta'$ 
27: end

```

---

### 3.1. Convergence Proof

With our reward function, the policy gradient is:

$$\nabla_\theta J(\pi_\theta) = \mathbb{E}_{\pi_\theta} \left[ \nabla_\theta \log \pi_\theta(a, D|s) \cdot (Q^\pi(s, a, D) \cdot (\alpha_m \cdot R_\tau) - \alpha_\varepsilon) \right] \quad (3)$$

where  $\nabla_\theta J(\pi_\theta)$  is the gradient of the objective function with respect to the policy parameters  $\theta$ .

The value function update, incorporating the time dimension  $D$  and our reward function, is:

$$L(\phi) = \mathbb{E}_{(s,a,D,r,s')} \left[ (Q_\phi(s, a, D) - (r + \gamma \mathbb{E}_{(a',D') \sim \pi_\theta} [V_{\phi'}(s') - \alpha \log \pi_\theta(a', D'|s')]))^2 \right] \quad (4)$$

where  $L(\phi)$  is the loss function for the value function update,  $r$  is the reward,  $\gamma$  is the discount factor, and  $V_{\phi'}(s')$  is the target value function.

The new policy parameter  $\theta$  update rule is:

$$\theta_{k+1} = \theta_k + \beta_k \mathbb{E}_{s \sim D, (a,D) \sim \pi_\theta} \left[ \nabla_\theta \log \pi_\theta(a, D|s) \cdot (Q_\phi(s, a, D) \cdot (\alpha_m \cdot R_\tau) - \alpha_\varepsilon - V_{\phi'}(s) + \alpha \log \pi_\theta(a, D|s)) \right] \quad (5)$$

where  $\beta_k$  is the learning rate at step  $k$ .

To analyze the impact of dynamically adjusting  $\alpha_m$  and  $\alpha_\varepsilon$ , we assume the following conditions. The dynamic adjustment rules specify that  $\alpha_m$  increases monotonically by a small increment  $\psi$  if the reward trend decreases over consecutive episodes. Its upper limit,  $\alpha_{max}$ , guarantees algorithmic convergence and prevents reward explosion. On the other hand,  $\alpha_\varepsilon$  decreases as defined.

The learning rate conditions must be satisfied, where  $\alpha_k$  and  $\beta_k$  adhere to the following equations [12]:

$$\sum_{k=0}^{\infty} \alpha_k = \infty, \quad \sum_{k=0}^{\infty} \alpha_k^2 < \infty \quad (6)$$

$$\sum_{k=0}^{\infty} \beta_k = \infty, \quad \sum_{k=0}^{\infty} \beta_k^2 < \infty \quad (7)$$

Assuming the critic estimates are unbiased:

$$\mathbb{E}[Q_\phi(s, a, D) \cdot (\alpha_m \cdot R_\tau) - \alpha_\varepsilon] = Q^\pi(s, a, D) \cdot (\alpha_m \cdot R_\tau) - \alpha_\varepsilon \quad (8)$$

Since  $R_\tau$  is a positive number within  $[0, 1]$ , its effect on  $Q^\pi(s, a, D)$  is linear and does not affect the consistency of the policy gradient.

The positive scaling condition states that as  $0 \leq R_\tau \leq 1$  and  $\alpha_m \geq 0$ ,  $\alpha_m$  only scales the reward without altering its sign. This scaling does not change the direction of the policy gradient but affects its magnitude. Additionally, a small offset  $\alpha_\varepsilon$  is used to accelerate training. This small offset does not affect the direction of the policy gradient but introduces a minor shift in the value function, which does not alter the overall policy update direction.

Under these conditions, MOSEAC will converge to a local optimum [24]:

$$\lim_{k \rightarrow \infty} \nabla_\theta J(\pi_\theta) = 0 \quad (9)$$

### 3.2. Lyapunov Stability

To analyze the stability of MOSEAC, we define a Lyapunov function  $V(t)$  and calculate its time derivative to ensure asymptotic stability:

$$V(t) = \frac{1}{2} \alpha_m(t)^2 + \sum_s [Q(s, a, D, \alpha_m) - Q^*(s, a, D)]^2 \quad (10)$$

where  $\alpha_m(t)$  varies with time,  $Q(s, a, D, \alpha_m)$  is the current Q-value ( $D$  is the duration of action  $a$ ), and  $Q^*(s, a, D)$  is the ideal Q-value.

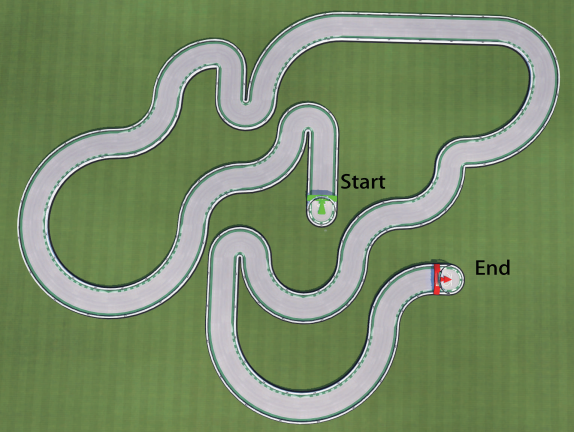


Figure 1: Top preview of the Trackmania track.

The time derivative of  $V(t)$  is:

$$\begin{aligned} \dot{V}(t) &= \alpha_m(t) \dot{\alpha}_m(t) \\ &+ \sum_s 2 [Q(s, a, D, \alpha_m) - Q^*(s, a, D)] \\ &\quad \dot{Q}(s, a, D, \alpha_m) \end{aligned} \quad (11)$$

Based on the linear growth model of  $\alpha_m$ :

$$\dot{\alpha}_m(t) = \begin{cases} k & \text{if } \alpha_m(t) < \alpha_{\max} \\ 0 & \text{if } \alpha_m(t) = \alpha_{\max} \end{cases} \quad (12)$$

Replacing in  $\dot{V}(t)$ :

$$\dot{V}(t) = \begin{cases} \alpha_m(t)k + \sum_s 2 [Q(s, a, D, \alpha_m) - Q^*(s, a, D)] \\ \quad \dot{Q}(s, a, D, \alpha_m), & \text{if } \alpha_m(t) < \alpha_{\max} \\ \sum_s 2 [Q(s, a, D, \alpha_m) - Q^*(s, a, D)] \\ \quad \dot{Q}(s, a, D, \alpha_m), & \text{if } \alpha_m(t) = \alpha_{\max} \end{cases} \quad (13)$$

Since  $\alpha_m(t) > 0$  and  $k > 0$ ,  $\dot{V}(t) > 0$  when  $\alpha_m(t) < \alpha_{\max}$ . However, when  $\alpha_m(t)$  reaches  $\alpha_{\max}$ ,  $\dot{V}(t) = 0$ , indicating that the system reaches a stable state.

#### 4. Experimental Setup

We validate our MOSEAC in a real-time racing game, Trackmania [1]. Figure 1 illustrates the testing environment. In Trackmania, players race to complete the track as quickly as possible. We employed the map developed by the TMRL [25] team for a direct comparison of MOSEAC’s performance against their SAC model. It is important to note that training and deploying a policy for this game can only happen in real time [20], ensuring the realism of the overall experiments.

For controlling the car in the game, Trackmania offers: • gas control; • brake control; and • steering. The action value includes the rate at which these controls are applied. The input

to the policy is the pixels as well as the numerical information shown on the heads-up display.

The reward system in the game is designed to encourage efficient path following: more rewards are given for covering more path points in a single move. This path is a series of evenly distributed points that collectively form the shortest route from the starting point to the end point of the racing game. This technique is consistent with the TMRL team’s methodology [25]. The game uses realistic car physics, but there is no car damage or crash detection. Further details are available in Table 1.

Table 1: Trackmania Environments Details		
State and action space of Trackmania		
	Data Space	Annotate
State Dimension	143	Details in Section 2
Car Speed	$(-1, 1)$	
Car Gear	$(-1, 1)$	RGB arrays
Wheel RPM	$(-1, 1)$	
RGB Image	$(64, 64, 3)$	
Action Dimension	4	
Gas Control	$(-1, 1)$	
Brake	$(-1, 1)$	
Yaw Control	$(-1, 1)$	
Control Rate	$(5, 30) Hz$	

To facilitate the agent’s comprehension of how the controls influence speed and acceleration, we feed 4 sequential frames (and the intervals between them) to a convolutional neural network (CNN), whose output is an embedding contributing to the state representation (see Figure 2). The CNN distills features, transforming the image data from a matrix of dimensions  $(4, 64, 64, 3)$  to a compact  $(128, 1, 1)$  matrix.

To evaluate the impact of our variable time step technique, we used the same visual-based navigation and task reward policy across the tested approaches, varying only the control rate. It is important to note that the task reward policy only includes time and disregards collisions.

Overall, our model inputs are the car’s speed, gear, and wheel RPM, the current step number in one episode, along with the two most recent actions taken, for a final 143-dimensional state.

#### 5. Experimental Results

We conducted experiments with MOSEAC, CTCO [11] and SEAC [26] on Trackmania for over 1320 hours<sup>1</sup>. These experiments were conducted on a I5-13600K computer with an NVIDIA RTX 4070 GPU. The final result video for MOSEAC is publicly available<sup>2</sup>, with 43.202 seconds to complete the test track.

<sup>1</sup>Our code is publicly available on GitHub: [https://github.com/alfaficia/TMRL\\_MOSEAC](https://github.com/alfaficia/TMRL_MOSEAC)

<sup>2</sup><https://youtu.be/1aQ0xSK55nk>

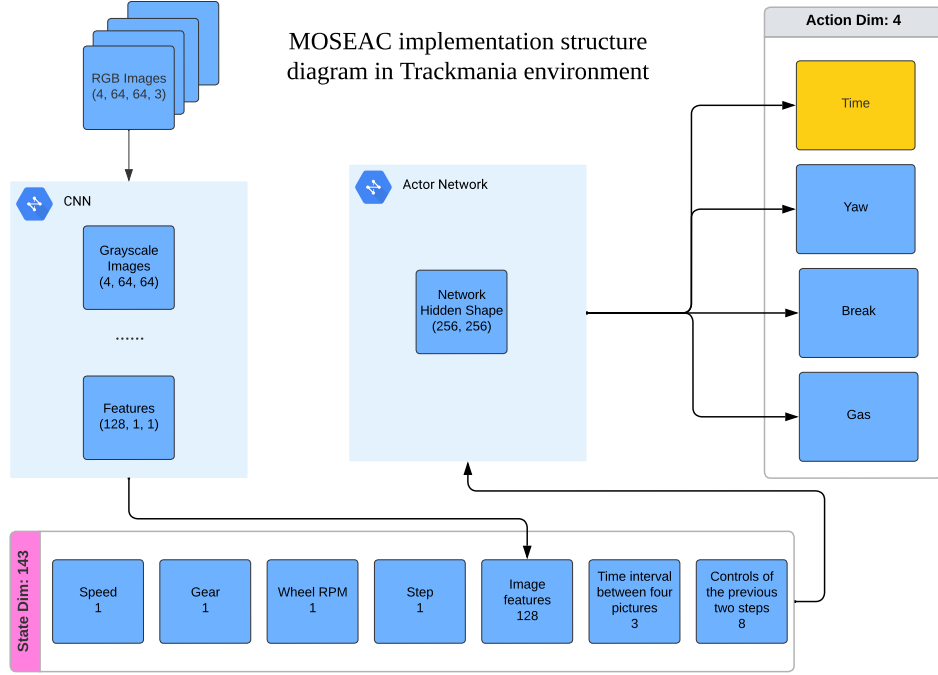


Figure 2: This is the implementation structure diagram of MOSEAC in the TrackMania environment. We use CNN to extract potential information in the environment and learn the extracted feature values based on rewards. The 143-dimensional state value and the 4-dimensional action value are shown in the figure. The time in the action value is not used for the current time step but for the next step.

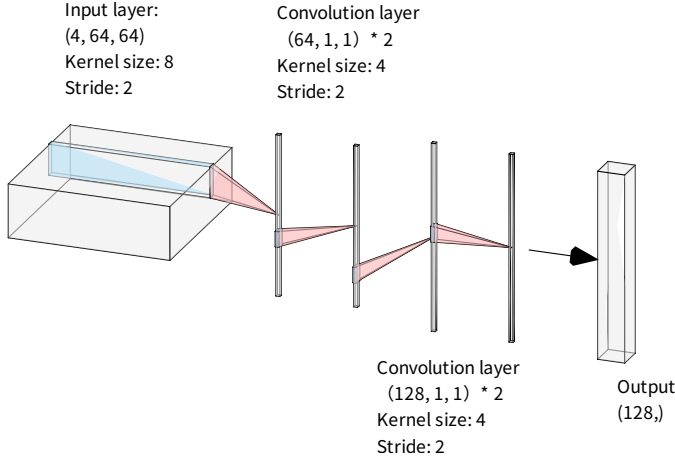


Figure 3: Our CNN structure diagram that we used to extract image features from the Trackmania video game. We convert RGB images into grayscale images and then input them into the CNN.

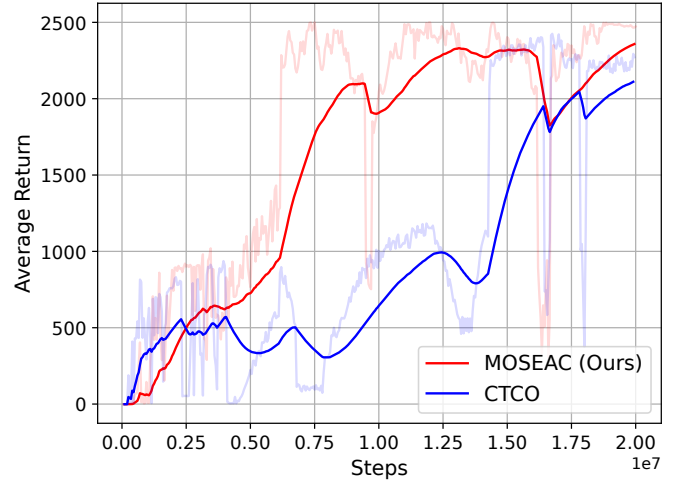


Figure 4: Training Progress of MOSEAC and CTCO: Average Return Over Time

Before discussing the performance of MOSEAC and CTCO, it is essential to provide some background context. In our previous work, the SEAC model policies were trained utilizing different hyperparameters [28]. These hyperparameters were explicitly tuned for SEAC, optimizing its performance in the given environment. Besides, the SAC model was trained by the TMRL team with a different set of hyperparameters tailored to their training technique [25]. Given these differences, directly comparing their training curves would be unfair; hence, we focus solely on the MOSEAC and CTCO training curves.

Reward signals are notably sparse in the environment set by the TMRL team. The reward is calculated based on the difference between the path coordinates after movement and the initial path coordinates, divided by 100 [25]. This sparse reward environment necessitates a very low-temperature coefficient alpha SAC [9], otherwise, the entropy component would dominate the reward. This insensitivity to reward signals can lead to poor training performance or even training failure. MOSEAC and CTCO are derived from SAC [27, 11], and they face similar constraints.

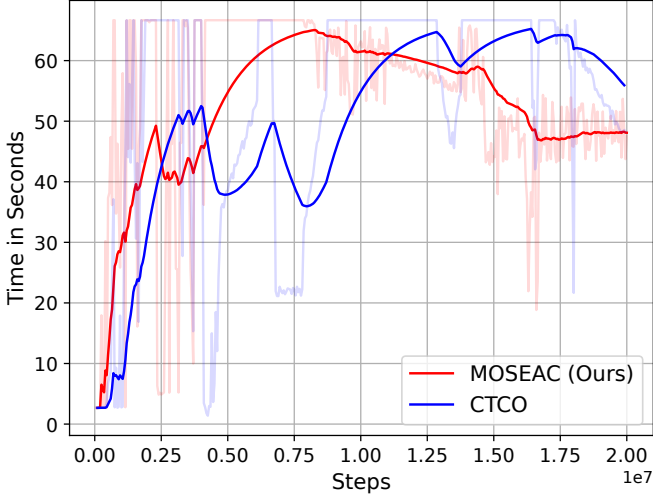


Figure 5: Training Progress of MOSEAC and CTCO: Time Consumption Over Steps

We have maintained this reward system to ensure a fair comparison with the TMRL team. Modifying the environment is not straightforward, as simply amplifying the reward signal may cause the agent to accumulate rewards rapidly, leading to overly optimistic estimates and unstable training. Such “reward explosion” can cause the agent to settle into local optima, neglecting long-term returns and reducing overall performance.

Using an adaptive temperature coefficient during training, we observed that the coefficient value becomes extremely low towards the end of the training. This results in a narrow distribution of actions, significantly slowing down the policy training and optimization process. This small temperature coefficient causes both MOSEAC and CTCO to have a slow training and optimization process.

Figure 4 demonstrates that MOSEAC reaches a high point at around 6 million steps, indicating initial training success. However, Figure 5 shows that after 6 million steps, MOSEAC required over 14 million additional steps to technique the optimal value. This indicates that MOSEAC and CTCO require substantial time for initial training and further optimization in a sparse reward environment.

Despite these challenges, MOSEAC exhibits better training efficiency than CTCO. MOSEAC adapts to the environment more quickly, maintaining a more stable learning curve. In contrast, CTCO, influenced by its adaptive  $\gamma$  mechanism, tends to favor smaller  $\gamma$  values, impairing long-term planning and significantly slowing down training. Furthermore, MOSEAC achieves a higher final reward than CTCO, showcasing its superior adaptability and efficiency in sparse reward settings.

Training in the Trackmania environment is real-time, and our 1320+ hours of training have shown that MOSEAC can handle complex, sparse reward environments, albeit requiring notable time investment. Therefore, if a direct comparison with our results, specifically regarding training speed within the same reward environment, is unnecessary, we recommend optimizing the reward signals in the TMRL Trackmania environment.

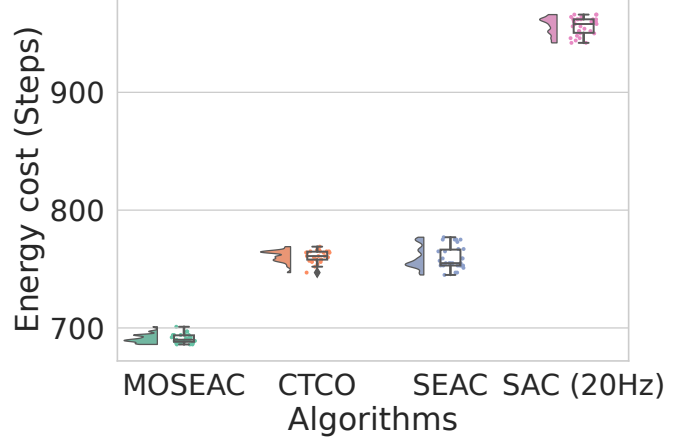


Figure 6: This figure compares the energy costs of four different algorithms: MOSEAC, CTCO, SEAC, and SAC (20Hz). The y-axis represents the energy cost in steps, while the x-axis lists the algorithms. The box plots demonstrate that MOSEAC has the lowest median energy cost, followed by SEAC, CTCO, and SAC (20Hz). This indicates that MOSEAC is the most energy-efficient among the four algorithms.

One possible optimization strategy could be to amplify the per-step reward signal appropriately. This adjustment theoretically allows for faster training of effective control policies, significantly enhancing training efficiency and saving substantial real-world time.

We compared the racetrack time (referred to as *time cost*) as well as the computational energy cost (in terms of the number of control steps) of MOSEAC with SEAC, CTCO, and SAC (20Hz) after training. Figure 6 illustrates the energy cost distribution and Figure 7 the time cost (lower is better in both cases). For both energy and time there is no overlap among the different methods, and the data follows a normal distribution (Shapiro-Wilk test of normality, see Table 2 and Table 4).

Using a paired sample T-test, MOSEAC showed lower energy in all of the trials compared with CTCO ( $t = -64.85$ ,  $df = 29$ ,  $p \ll 0.001$ ), SEAC ( $t = -35.90$ ,  $df = 29$ ,  $p \ll 0.001$ ), and SAC ( $t = -196.35$ ,  $df = 29$ ,  $p \ll 0.001$ ). The statistics for the energy cost measures are presented in Table 3. Similarly, MOSEAC showed lower race time in all of the trials compared with CTCO ( $t = -55.67$ ,  $df = 29$ ,  $p \ll 0.001$ ), SEAC ( $t = -32.92$ ,  $df = 29$ ,  $p \ll 0.001$ ), and SAC ( $t = -41.06$ ,  $df = 29$ ,  $p \ll 0.001$ ). The statistics for the time cost measures are presented in Table 5.

Table 2: Test of Normality (Shapiro-Wilk) - Energy cost difference

			W	p
MOSEAC	-	CTCO	0.947	0.142
MOSEAC	-	SEAC	0.948	0.150
MOSEAC	-	SAC (20Hz)	0.956	0.242

The improved performance of MOSEAC over SEAC, CTCO, and SAC (20Hz) can be attributed to its reward function and the integration of a state variable. SEAC uses a linear reward function that independently combines task reward, energy penalty,



Table 3: Energy cost descriptives

	N	Mean	SD	SE	COV
MOSEAC	30	690.800	3.652	0.667	0.005
CTCO	30	760.933	4.989	0.911	0.007
SEAC	30	759.467	9.508	1.736	0.013
SAC (20Hz)	30	956.133	7.482	1.366	0.008

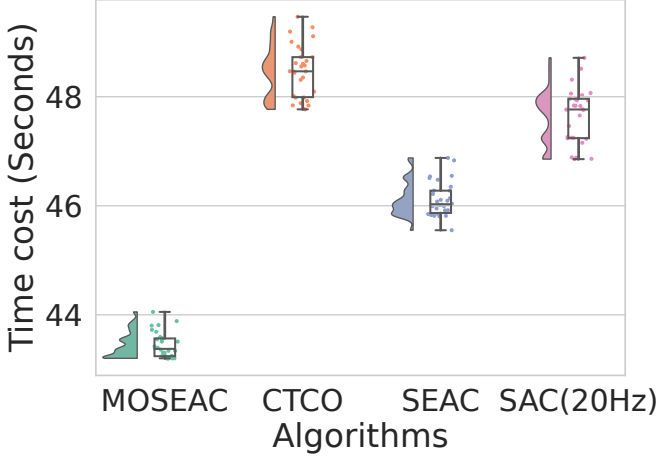


Figure 7: This figure compares the time costs of four different algorithms: MOSEAC, CTCO, SEAC, and SAC (20Hz). The y-axis represents the time cost in seconds, while the x-axis lists the algorithms. The box plots reveal that MOSEAC has the lowest median time cost, indicating faster task completion compared to the other algorithms. CTCO, SEAC, and SAC (20Hz) demonstrate higher median time costs, with MOSEAC outperforming them in terms of time efficiency.

and time penalty. In contrast, MOSEAC employs a multiplicative relationship between task and time-related rewards. This non-linear interaction enhances the reward signal, especially when task performance and time efficiency are high, thereby naturally balancing these factors. By keeping the energy penalty separate, MOSEAC retains flexibility in tuning without complicating the relationship between time and task rewards. This design allows MOSEAC to guide the agent’s decisions more effectively, resulting in improved energy efficiency and faster task completion in practical applications.

## 6. Conclusions

In this paper, we introduced and evaluated the Multi-Objective Soft Elastic Actor-Critic (MOSEAC) algorithm, demonstrating its superior performance compared to CTCO, SEAC, and SAC (20Hz) in the sparse reward environment created by the TMRL team in the Trackmania game. MOSEAC features an innovative reward function that combines task rewards and time-related rewards, enhancing the reward signal when both task performance and time efficiency are high. This non-linear interaction balances these factors, leading to improved energy efficiency and task completion speed.

To prevent reward explosion, we introduced an upper limit ( $\alpha_{max}$ ) for the hyperparameter  $\alpha_m$ , ensuring convergence and

Table 4: Test of Normality (Shapiro-Wilk) - Time cost difference

			W	p
MOSEAC	-	CTCO	0.954	0.222
MOSEAC	-	SEAC	0.963	0.367
MOSEAC	-	SAC (20Hz)	0.968	0.478

Table 5: Time cost descriptives

	N	Mean	SD	SE	COV
MOSEAC	30	43.441	0.237	0.043	0.005
CTCO	30	48.463	0.481	0.088	0.010
SEAC	30	46.117	0.317	0.058	0.007
SAC (20Hz)	30	47.636	0.510	0.093	0.011

stability, validated utilizing a Lyapunov model. The boundedness analysis confirmed that  $\alpha_m$  remains within the defined limits, maintaining the strength of the reward function and ensuring the robustness and reliability of the learning process.

Our experiments in the Trackmania environment, conducted over 1300 hours, validated these enhancements, showcasing MOSEAC’s robustness and efficiency in real-world applications. The recorded best time for MOSEAC is 43.202 seconds, significantly faster than the other algorithms.

Building on MOSEAC’s success, our future work will focus on extending the principles of variable time step algorithms to other RL frameworks, such as Hierarchical Reinforcement Learning (HRL). This extension aims to address the complexities of long-term planning tasks more efficiently, further improving the adaptability and performance of RL algorithms in diverse and challenging environments, which brings benefits for solving complex problems by RL utilizing real robot systems.

## References

- [1] 2023, U.T., 2023. Trackmania main page. <https://www.ubisoft.com/en-us/game/trackmania/trackmania>.
- [2] Amin, S., Gomrokchi, M., Aboutaleb, H., Satija, H., Precup, D., 2020. Locally persistent exploration in continuous control tasks with sparse rewards. arXiv preprint arXiv:2012.13658.
- [3] Bainomugisha, E., Carreton, A.L., Cutsem, T.v., Mostinckx, S., Meuter, W.d., 2013. A survey on reactive programming. ACM Computing Surveys (CSUR) 45, 1–34.
- [4] Bregu, E., Casamassima, N., Cantoni, D., Mottola, L., Whitehouse, K., 2016. Reactive control of autonomous drones, in: Proceedings of the 14th Annual International Conference on Mobile Systems, Applications, and Services, pp. 207–219.
- [5] Chen, Y., Wu, H., Liang, Y., Lai, G., 2021. Varlenmarl: A framework of variable-length time-step multi-agent reinforcement learning for cooperative charging in sensor networks, in: 2021 18th Annual IEEE International Conference on Sensing, Communication, and Networking (SECON), IEEE. pp. 1–9.
- [6] Chow, Y., Nachum, O., Duenez-Guzman, E., Ghavamzadeh, M., 2018. A lyapunov-based approach to safe reinforcement learning. Advances in neural information processing systems 31.
- [7] Cui, W., Jiang, Y., Zhang, B., 2022. Reinforcement learning for optimal primary frequency control: A lyapunov approach. IEEE Transactions on Power Systems 38, 1676–1688.

- [8] Dietterich, T.G., 2000. Hierarchical reinforcement learning with the maxq value function decomposition. *Journal of artificial intelligence research* 13, 227–303.
- [9] Haarnoja, T., Zhou, A., Abbeel, P., Levine, S., 2018a. Soft actor-critic: Off-policy maximum entropy deep reinforcement learning with a stochastic actor, in: *International conference on machine learning*, PMLR. pp. 1861–1870.
- [10] Haarnoja, T., Zhou, A., Hartikainen, K., Tucker, G., Ha, S., Tan, J., Kumar, V., Zhu, H., Gupta, A., Abbeel, P., et al., 2018b. Soft actor-critic algorithms and applications. *arXiv preprint arXiv:1812.05905*.
- [11] Karimi, A., Jin, J., Luo, J., Mahmood, A.R., Jagersand, M., Tosatto, S., 2023. Dynamic decision frequency with continuous options, in: *2023 IEEE/RSJ International Conference on Intelligent Robots and Systems (IROS)*, IEEE. pp. 7545–7552.
- [12] Konda, V., Tsitsiklis, J., 1999. Actor-critic algorithms. *Advances in neural information processing systems* 12.
- [13] Lee, J., Lee, B.J., Kim, K.E., 2020. Reinforcement learning for control with multiple frequencies. *Advances in Neural Information Processing Systems* 33, 3254–3264.
- [14] Li, S., Wang, R., Tang, M., Zhang, C., 2019. Hierarchical reinforcement learning with advantage-based auxiliary rewards. *Advances in Neural Information Processing Systems* 32.
- [15] Lyapunov, A.M., 1992. The general problem of the stability of motion. *International journal of control* 55, 531–534.
- [16] Majumdar, R., Mathur, A., Pirron, M., Stegner, L., Zufferey, D., 2021. Paracosm: A test framework for autonomous driving simulations, in: *International Conference on Fundamental Approaches to Software Engineering*, Springer International Publishing Cham. pp. 172–195.
- [17] Metelli, A.M., Mazzolini, F., Bisi, L., Sabbioni, L., Restelli, M., 2020. Control frequency adaptation via action persistence in batch reinforcement learning, in: *International Conference on Machine Learning*, PMLR. pp. 6862–6873.
- [18] Monfared, M.S., Monabbati, S.E., Kafshgar, A.R., 2021. Pareto-optimal equilibrium points in non-cooperative multi-objective optimization problems. *Expert Systems with Applications* 178, 114995.
- [19] Park, S., Kim, J., Kim, G., 2021. Time discretization-invariant safe action repetition for policy gradient methods. *Advances in Neural Information Processing Systems* 34, 267–279.
- [20] Ramstedt, S., Pal, C., 2019. Real-time reinforcement learning. *Advances in neural information processing systems* 32.
- [21] Sharma, S., Srinivas, A., Ravindran, B., 2017. Learning to repeat: Fine grained action repetition for deep reinforcement learning. *arXiv preprint arXiv:1702.06054*.
- [22] Shin, K., McKay, N., 1985. Minimum-time control of robotic manipulators with geometric path constraints. *IEEE Transactions on Automatic Control* 30, 531–541.
- [23] Silver, D., Huang, A., Maddison, C.J., Guez, A., Sifre, L., Van Den Driessche, G., Schrittwieser, J., Antonoglou, I., Panneershelvam, V., Lanctot, M., et al., 2016. Mastering the game of go with deep neural networks and tree search. *nature* 529, 484–489.
- [24] Sutton, R.S., Barto, A.G., 2018. *Reinforcement learning: An introduction*. MIT press.
- [25] tmrl, 2023. tmrl main page. <https://github.com/trackmania-rl/tmrl>.
- [26] Wang, D., Beltrame, G., 2024a. Deployable reinforcement learning with variable control rate. *arXiv preprint arXiv:2401.09286*.
- [27] Wang, D., Beltrame, G., 2024b. Moseac: Streamlined variable time step reinforcement learning. *arXiv preprint arXiv:2406.01521*.
- [28] Wang, D., Beltrame, G., 2024c. Reinforcement learning with elastic time steps. *arXiv preprint arXiv:2402.14961*.
- [29] Wurman, P.R., Barrett, S., Kawamoto, K., MacGlashan, J., Subramanian, K., Walsh, T.J., Capobianco, R., Devlic, A., Eckert, F., Fuchs, F., et al., 2022. Outracing champion gran turismo drivers with deep reinforcement learning. *Nature* 602, 223–228.



include RL, computer vision, and robotics.



**Dong Wang** received his bachelor's degree in electronic engineering from the School of Aviation, Northwestern Polytechnical University (NWPU), Xi'an, China, in 2017. He is pursuing his Ph.D. in the Department of Software Engineering at Polytechnique Montreal, Montreal, Canada. His research interests include RL, computer vision, and robotics.

**Giovanni Beltrame** received the Ph.D. degree in computer engineering from Politecnico di Milano, Milan, Italy, in 2006. He worked as a Microelectronics Engineer with the